

# Grating-based surface-normal optoelectronic interconnects on Si substrate

Feiming Li, Michael Dubinovsky, Oleg Ershov, Linghui Wu, Ting Li, Suning Tang and Ray T. Chen

Microelectronics Research Center  
Department of Electrical and Computer Engineering  
The University of Texas at Austin, Austin, TX 78758

## ABSTRACT

We report in this paper the surface-normal input and output grating couplers for 1-to-many fanouts aiming at optical clock signal distribution application. For wafer-scale interconnects, surface-relief polygonal gratings with a  $1\ \mu\text{m}$  period ( $0.5\ \mu\text{m}$  feature size) were fabricated using reactive ion beam etching (RIE). Surface-normal input and output coupling schemes were carried out with an combined coupling efficiency of 65%. Employment of substrate modes in silicon greatly releases the required grating spacing for the demonstrated two-way surface-normal coupling. 7.5 GHz 1-to-4 clock signal distribution operating at  $1.3\ \mu\text{m}$  was demonstrated with a signal to noise ratio as high as 60 dB. Generalization of 1-to-many fanout can be realized by implementing a polygonal grating with an equivalent number of facets. For board level optical clock signal distribution system, a preliminary result using a parallelogramic grating to couple surface-normal input light into polyimide waveguide is also reported.

Keyword: optoelectronic interconnect, waveguide grating coupler, polyimide waveguide

## 1. INTRODUCTION

With the advent of higher clock speeds and distributed multiprocessor computer architecture, a great deal of interest has arisen in synchronously distributing a clock signal over all the processors in a computer with an acceptable clock skew<sup>1</sup>. Unfortunately, at clock speeds above 500 MHz, a synchronous global clock distribution system is very difficult to attain using electrical interconnects due to skin-effect induced losses, impedance-mismatch due to large fanouts, and RLC-related charging times which are detrimental for the realization of such an electrically interconnected high speed system. Because of the high bandwidth inherent in optical signals, various guided wave optical clock distribution schemes have been investigated to alleviate such a problem. Photopolymer-based multiplexed volume holograms<sup>2</sup> have been employed to achieve massive fanouts up to 59/node<sup>3</sup>. Surface relief materials have also been employed by using different diffraction orders of surface relief gratings<sup>4</sup> to achieve the required fanout. Due to the nature of non-multiplexibility, a surface relief grating is primarily employed as a 1-to-1 interconnect device with a relatively low interconnectivity<sup>5</sup>. For 1-to-many fanout optical interconnects employing surface relief material with a single fanout node, a new device configuration is needed to solve this problem.

## 2. EXPERIMENTS AND RESULTS

### 2.1. Wafer level interconnection

In this section, we demonstrate the first Si-based polygonal gratings for 1-to-many fanouts with a surface normal configuration. A linear grating was converted into a polygonal format with the required grating vector for each predestined fanout direction. A central polygonal input coupling grating and surrounding linear output coupling gratings were employed to provide the desired optical clock signal distribution. As shown in Fig.1, equivalent optical paths (and thus minimized clock skew) are provided through this approach. A double-side polished Si wafer is used to minimize the surface scattering losses as the signal travels through the bulk of the Si wafer. The number of fanouts is determined by the total facets associated with the polygonal grating needed to realize the 1-to-many clock signal distribution. The basic coupling configuration is illustrated in the inset of Fig.1 which provides a substrate guided wave with a bouncing angle  $\Theta_t$  within the silicon substrate from the surface normal incident direction. For an operating wavelength of  $1.3 \mu\text{m}$  with air as the cladding medium, the critical angle for total internal reflection is less than  $16.6^\circ$  which makes a grating period of  $1 \mu\text{m}$  applicable for this demonstration. Note that the zigzag bouncing mode described in this paper is the substrate guided waves which were defined as "substrate modes" in the conventional terminology of integrated optics<sup>6</sup>. Employment of these modes significantly releases the grating spacing requirement for surface-normal coupling and therefore facilitates the fabrication process. Both the central polygonal and linear output gratings have a period of  $1 \mu\text{m}$ , allowing optical signals to be efficiently coupled into and out of the Si wafer substrate guided modes in the surface normal direction.

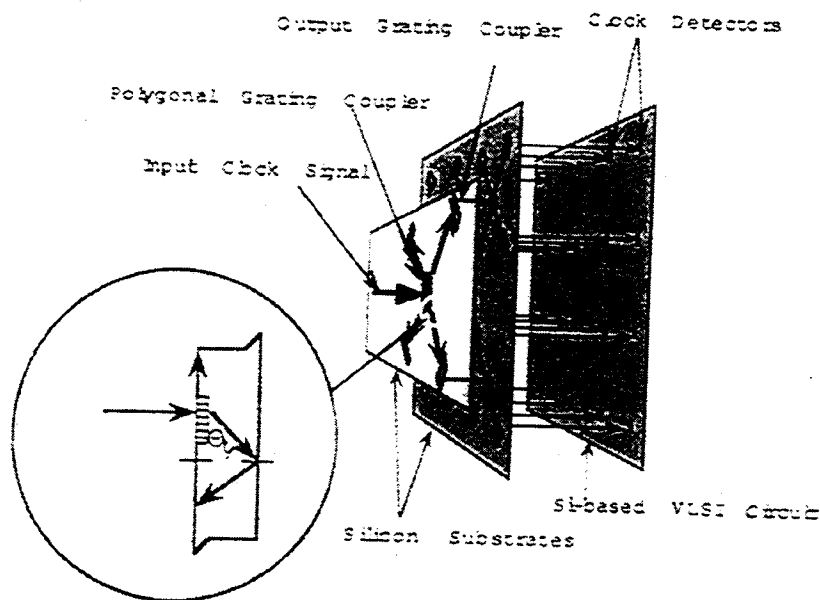


Fig.1 Schematic of Si-based optical clock distribution system using Si-based polygonal gratings and substrate guided waves with surface-normal coupling configuration

In this paper, 1-to-4 fanouts were experimentally demonstrated. A photoresist pattern was used as the masking material for the etch process. The first stage of the RIE process was the removal of SiO<sub>2</sub> layer using CF<sub>4</sub> gas and the second stage was the formation of the grating microstructure using RIE with Cl<sub>2</sub> and He as the active gasses with flow rates of 30.0 cm<sup>3</sup>/sec and 94.2 cm<sup>3</sup>/sec, respectively. In using this technique with 1 μm period gratings, careful process control must be used to insure that the photoresist is removed all the way down to the wafer in the exposed stripes of the grating.

To characterize etch rate of RIE samples, diffraction efficiencies of grating samples were measured as a function of etch time for three different wavelengths: 0.632, 1.06, and 1.32 μm. This was done to determine the actual depth of the fabricated gratings. An accurate evaluation of the grating depth at various etch times was determined using the multiple wavelength approach<sup>7,8</sup>. Based on the etch rate data, 1-to-4 fanout gratings were successfully fabricated using RIE. With an operating wavelength at 1.3 μm, the grating with 1 μm period will be sufficient to provide the required TIR beams within silicon substrate for the proposed optical clock signal distribution. The microstructure of the fabricated 1-to-4 square grating is further illustrated in Fig.2(a) where equal partitions of the real estate of the gratings are clearly indicated. An SEM photograph containing a linear section of a typical 1-to-many fanout grating attained with this technique is further illustrated in Fig.2(b). An etching depth of 0.5 μm was experimentally confirmed for both square and hexagonal gratings. 1-to-4 fanouts were realized using these devices which convert surface-normal incident beams to substrate guided waves with a bouncing angle of 21.6°. A 1.3 μm Nd:YAG laser beam with a circular polarization was coupled into the Si substrate through the center polygonal grating. Fig.3 is a three-dimensional photograph of a 1-to-4 fanout device in operation. The central peak of Fig.3 is corresponding to the 0th order beam, four others to the 1st order output diffracted beams. The modulated 1.3 μm laser beam is collimated and then coupled by a lens with a focal length of 100 mm surface-normally into the 1-to-4 surface-normal fanout grating as indicated in Fig.1. The four zigzag substrate guided waves were then coupled out through four separate output gratings. Note that each surface normal fanout beam shown in Fig.3 contains +1 and -1 diffraction orders from two separate triangle gratings having the same grating vector. In the considered case, 65% of the light incident on the polygonal grating is coupled into the substrate. The peak intensities of output beams are about 20% of peak intensity of the 0th order undiffracted beam. The intensity uniformity of the four surface-normal fanout beams were found to be primarily determined by the quality of grating and the accuracy of the position adjustment of the incident beam with respect to the central square grating. The diffraction efficiency uniformity for 1-to-4 fanout beams was measured to be within 1 dB, i.e., 10%, fluctuation. The scenario with 1-to-many interconnects having an arbitrary fanout number can be realized by constructing a corresponding polygonal grating with an equivalent number of facets. The upper limit of fanout is determined by the near field and far field diffraction patterns when a light beam interacts with the triangular grating with a tip angle of  $2\pi/n$ , where  $n$  is the number of fanout. Due to the page limitation, the theoretical details of this investigation will be presented in a separate publication in the near future.

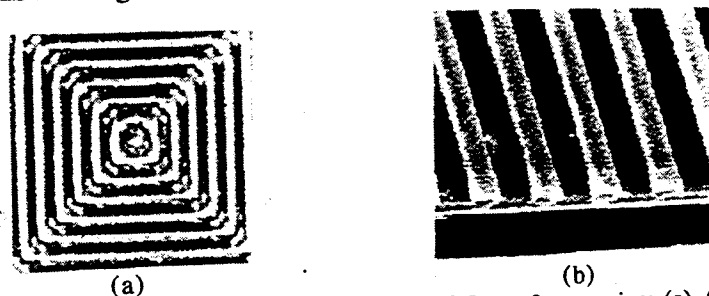


Fig.2 Microstructures of polygonal gratings with 0.5 μm feature size; (a) A square grating for 1-to-4 fanout, (b) Scanning electron microscope (SEM) picture of a section of a polygonal grating with 1 μm feature having an etched depth of 0.5 μm.

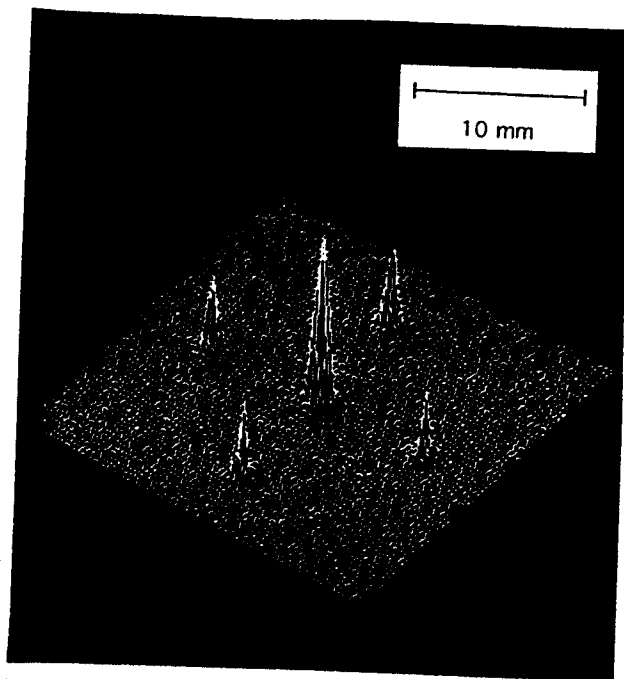


Fig.3 Three-dimensional intensity profile of the Si-based 1-to-4 surface-normal fanout; the center peak is corresponding to the 0th diffraction order of the incident beam (Fig.1) and the four other equally separated ones are the surface normal fanout beams coupled out from the four output Si-based surface relief gratings. Power fluctuation of the four fanout beams is within 1dB.

We performed diffraction efficiency measurements for incident beams with transverse electric (TE) and transverse magnetic (TM) polarization states. Fig.4 depicts the measured diffraction efficiencies of TE and TM incident beams as a function of the grating groove depths. Note that the data presented in Fig.4 provide us with the net diffraction efficiency for the incident beam with an arbitrary intensity and beam polarization through appropriately decomposing the ratio of TE and TM polarized incident beams. The ratio of  $\frac{\eta_{TE}}{\eta_{TM}}$  fits well with the relationship  $\frac{\eta_{TE}}{\eta_{TM}} \propto \left(\frac{d}{\lambda}\right)^2$ , where  $d$  is the groove depth,  $\lambda$  is the wavelength and  $\eta_{TE}$  and  $\eta_{TM}$  are diffraction efficiencies for TE and TM waves, respectively. Obviously, the same relation is kept if one takes  $\left(\frac{d}{\lambda}\right)$  in stead of  $\left(\frac{d}{\lambda}\right)$ . Such a statement is justifiable in reference to 9 and 10. Note that, in deriving Fig.4, one transmission grating (the input coupler) and one reflection grating (the output coupler) are involved for each measured data.

The optical clock signal coupled into the Si substrate was generated using an HP 8703A Lightwave component analyzer and detected using an Epitax ETX-25B high speed InGaAs PIN-photodiode. This particular prototype device was fabricated in a single lithographic step followed by an RIE step with the etch time set to produce a grating depth of 0.3  $\mu\text{m}$ , optimizing the coupling efficiency into the substrate.

The detected signal at the output was analyzed using a sampling scope and a microwave spectrum analyzer. The measured 7.5 GHz clock speed shown in the analyzer is further illustrated in Fig.5. To understand the bandwidth coverage of the optical clock distribution system, we further measured the frequency response of the photodiode. The result concludes that the 7.5 GHz was due to the bandwidth of the photodiode rather than the optical clock signal distribution system itself.

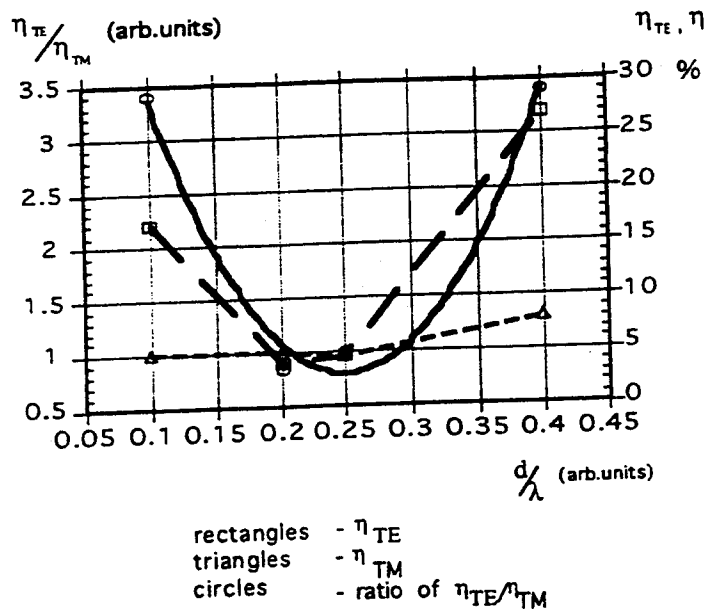


Fig.4 Measured diffraction efficiencies of  $\eta_{TE}$  and  $\eta_{TM}$  as a function of the grating groove depth using different beam polarizations as parameters. The ratio of  $\eta_{TE}/\eta_{TM}$  is also provided, which follows the  $(d/\Lambda)^2$  and  $(d/\lambda)^2$  dependence ( $d$ =grating groove depth,  $\Lambda$ =grating period and  $\lambda$ =wavelength).

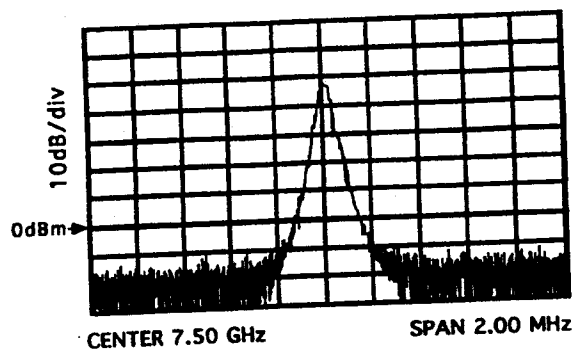


Fig.5 7.5 GHz clock signal detected at the surface-normal direction from one of the fanout gratings (Fig.1).

## 2.2. Board level interconnection

In this section, we present the demonstration of the preliminary result on the surface-normal input waveguide grating coupler for a proposed board level optical clock signal distribution system. In this project, a layer of polyimide optical channel waveguide will be inserted to the electronic board. The surface normal input optical clock signal was coupled by a linear grating into the channel waveguide. A Y-branch can be used to divide the clock signal into multiple recipients. In contrary to the above square groove gratings, a special parallelogramic-shape grating groove was used for unidirectional coupling. Previous theoretical results showed that this kind of groove profile has the advantage of higher coupling efficiency compared with square or triangular grating grooves<sup>11</sup>. Because of the linear dimension of the interconnect board (30 cm), a Si substrate can not be used. Instead, we chose polyimide waveguide media

which can be coated onto a PC board. Polyimides are widely used in semiconductor fabrication as an interlayer dielectric materials. They have the advantage of excellent chemical resistance and thermal stability at temperature as high as 400 °C and therefore compatible with the semiconductor fabrication processes.

In this paper, a polyimide waveguide layer on glass substrate was used as a demo. An A600 primer layer was spin-coated first on the substrate with a spin speed of 5000 rpm, and prebaked at 90 °C for 60 seconds. The Amoco polyimide 9120D was then spin-coated with a speed of 2000 rpm. A final curing at 260 °C in nitrogen atmosphere was carried out for more than three hours. Typical thickness of the waveguide was 7 μm. The planar waveguide has also been successfully fabricated on Si substrate by inserting a 9020D cladding layer between the 9120D guided layer and the Si substrate.

In order to fabricate the grating coupler by RIE, a thin aluminum metal mask was deposited on top of the polyimide-based planar guide. The schematic diagram for the fabrication process is shown in Fig.6. First, a 500 Angstroms aluminum layer was coated on top of the waveguide by electron beam evaporation, followed by a layer of 5206E photoresist with spin speed of 3000 rpm. The grating patterns on photoresist was recorded by interfering two beam of the  $\lambda=442\text{nm}$  He-Cd laser line. In order to record a grating with a period of  $\Lambda$ , the cross angle  $\theta$  of the two interference beams is determined through the formular of  $\sin(\theta / 2) = (\lambda / \Lambda)$ . After the sample has been developed, a postbake at 120 °C for 30 minutes was followed. To transfer the photoresist grating patterns to aluminum, we used RIE to etch the aluminum in the opening window of the photoresist pattern. The gases used were  $\text{BCl}_3/\text{SiCl}_4$  with a pressure of 20 millitorr. However, it was found that there were still some photoresist residuals in the grating groove which could block the aluminum RIE process. In order to clean these residuals, an additional step of RIE etching using oxygen was applied before removing the Al layer. To form the tilted grating pattern on the polyimide waveguide, we used a RIE process with a low oxygen pressure of 10 millitorr to transfer the grating pattern on aluminum layer to the polyimide layer. In order to get the tilted profile, a Faraday cage<sup>12</sup> was used. The sample inside the cage was placed at a tilted angle of 40 degrees with respect to the incoming oxygen ions. The final step was to remove the aluminum mask by another step of RIE process.

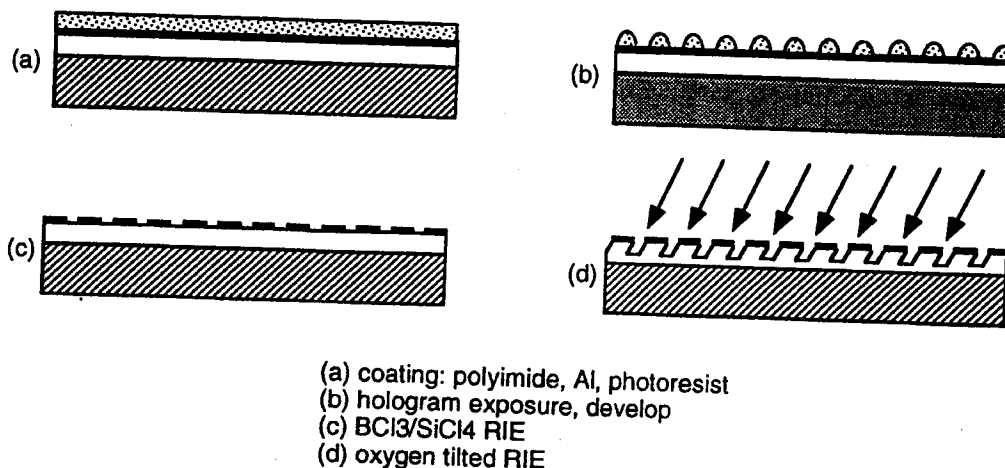


Fig.6 The schematic diagram for the fabrication of tilted grating on polyimide waveguide.

The schematic of coupling a surface-normal input light into waveguide using the device fabricated is shown in Fig.7(a), together with an experimental photograph in Fig.7(b). Here, an unpolarized 632.8nm He-Ne laser was used as surface-normal incident light. The coupling to the planar waveguide with the unidirectional propagation can be clearly observed with a measured efficiency of 5%. This is our first device which realized the surface-normal waveguide input coupling. Further studies of the grating parameters in order to increase the coupling efficiency are under investigation.

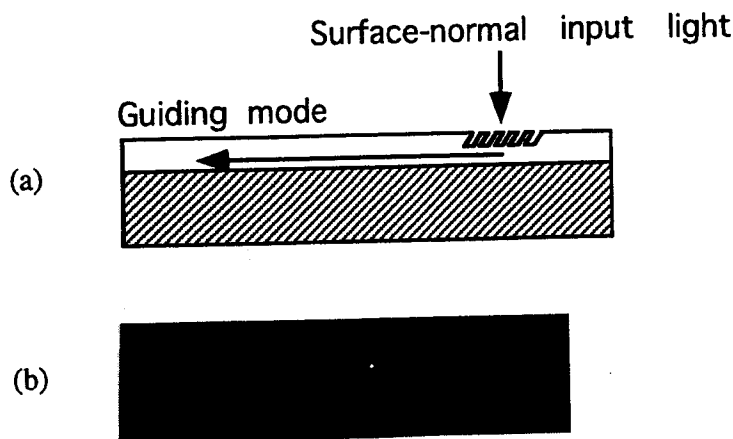


Fig.7 (a) The schematic of coupling a surface-normal input light into waveguide using the tilted grating. (b) The experimental photograph of coupling a surface-normal input 632.8 nm He-Ne light into the polyimide waveguide.

### 3. CONCLUSION

In conclusion, we have demonstrated a novel architecture for optical clock signal distribution. Employment of substrate modes instead of conventional guided mode significantly releases the grating spacing for the required phase-matching condition. Surface relief gratings on silicon substrate with multiple grating vectors were fabricated using square patterns. 1-to-4 fanouts with uniform intensities were demonstrated at 1.3  $\mu\text{m}$ . Using this method, a prototype device with an input/output coupling efficiency of 65% having a measured 7.5 GHz clock speed with interconnection distance of up to 8 cm was demonstrated. For the board level clock signal distribution applications, a parallelogramic grating coupler realized the unidirectional input coupling of light into the polyimide waveguide.

### 4. ACKNOWLEDGMENTS

This research is sponsored by ONR, BMDO, ARPA's Center of Optoelectronics Science Technology (COST), Radiant Research, Inc. and the ATP program of the state of Texas. We are grateful to Luke Graham and Jiten Sarathy for their helps in various stages of the experiment. The authors thank Professor Joe Campbell for his assistance in speed measurement.

### 5. REFERENCES

1. S.Koh, H.Carter, J.Boyd, "Synchronous global clock distribution on multichip modules using optical waveguides", *Opt.Eng.*, vol.33, no.5, pp.1587-1595, 1994.
2. Suning Tang, Ray T.Chen, "1-to-42 optoelectronic interconnection for intra-multichip-module clock signal distribution", *Appl. Phys. Lett.*, vol.66, no.22, pp.2931-2933, 1994.

3. Ray T.Chen, "Polymer-based photonic integrated circuits", *Opt.& Laser Techn.*, vol.25, no.6, pp.347-365, 1993.
4. S.Walker, J.Jahns, L.Li, W.Mansfield et al, "Design and fabrication of high efficiency beam splitters and beam deflectors for integrated planar micro-optic systems", *Appl.Opt.*, vol.32, no.14, pp.2494 - 2501, 1993.
5. J.E. Morris, M.R. Feldman, W.H. Welch, M. Nakkar, H. Yang, J. Childers, Y. Raja, I. Turlik, G. Adema, P. Magill and E. Yung, "Prototype optically interconnected multichip module based on computer generated hologram technology", *Proc. SPIE.*, Vol.1849, pp.48-58, 1994.
6. P. K. Tien, "Light waves in thin films and integrated optics", *Appl. Opt.*, vol.10, pp.2395-2413, 1971.
7. K.Rastani, W.Hubbard, "Alignment and fabrication tolerances of planar gratings for board-to-board optical interconnects", *Appl.Opt.*, vol.31, no.23, pp.4863-4870, 1992.
8. M.Josse, D.Kendall, "Rectangular profile diffraction grating from single crystal Si", *Appl.Opt.*, vol.19, no.1, pp.72-76, 1980.
9. T.Gaylord, M.Moharam, "Analysis and applications of optical diffraction by gratings", *Proc.IEEE*, vol.73, no.5, pp.894-934, 1985.
10. D.Brundrett, E.Glystis, T.Gaylord, "Homogeneous layer models for high-spatial-frequency dielectric surface-relief gratings", *Appl.Opt.*, vol.33, no.13, pp.2695-2706, 1994.
11. M.Li, S.J.Sheard, "Waveguide couplers using parallelogramic-shaped blazed gratings", *Opt. Comm.*, vol. 109, pp. 239-245, 1994.
12. G.D.Boyd, L.A.Coldren, F.G.Storz, "Directional reactive ion etching at oblique angles", *Appl. Phys. Lett.*, vol. 36, no. 7, pp. 583-585, 1980.